Available online at www.sciencedirect.com
ScienceDirect
Advances in Space Research 44 (2009) 340–347
ADVANCES IN SPACE RESEARCH (a COSPAR publication)
www.elsevier.com/locate/asr

Clues on black hole feedback from simulated and observed X-ray properties of elliptical galaxies

S. Pellegrini [a,*], L. Ciotti [a], J.P. Ostriker [b]

[a] Astronomy Department, Bologna University, via Ranzani 1, 40127 Bologna, Italy
[b] Princeton University Observatory, Peyton Hall, Princeton, NJ 08544, USA

Received 8 January 2009; received in revised form 27 March 2009; accepted 12 April 2009

Abstract

The centers of elliptical galaxies host supermassive black holes that significantly affect the surrounding interstellar medium through feedback resulting from the accretion process. The evolution of this gas and of the nuclear emission during the galaxies' lifetime has been studied recently with high-resolution hydrodynamical simulations. These included gas cooling and heating specific for an average AGN spectral energy distribution, a radiative efficiency declining at low mass accretion rates, and mechanical coupling between the hot gas and AGN winds. Here, we present a short summary of the observational properties resulting from the simulations, focussing on (1) the nuclear luminosity; (2) the global luminosity and temperature of the hot gas; (3) its temperature profile and X-ray brightness profile. These properties are compared with those of galaxies of the local universe, pointing out the successes of the adopted feedback and the needs for new input in the simulations.

Keywords: Elliptical galaxies; AGN outbursts; ISM; X-rays: galaxies

1. Introduction

Supermassive black holes (MBHs) at the centers of bulges and elliptical galaxies played an important role during galaxy formation and evolution, as revealed by remarkable correlations between their masses and some host galaxy properties (e.g., Ferrarese and Merritt, 2000; Gebhardt et al., 2000) and by many studies (e.g., Merloni et al., 2004; Sazonov et al., 2005; Di Matteo et al., 2005; Hopkins et al., 2006; Kormendy et al., in press). An important aspect of the coevolution process is the interaction between the energy emitted by the accreting MBH and a galactic interstellar medium (ISM) continuously replenished by normal stellar mass losses. In the absence of feedback from a central MBH, this ISM develops a flow directed towards the galactic center, accreting $\gtrsim 1 M_\odot\ \mathrm{yr}^{-1}$ in a process similar to a "cooling flow" (e.g., Ciotti et al., 1991; David et al., 1991; Pellegrini and Ciotti, 1998). Therefore a few basic questions arise: (1) what is the fate of the large amounts of gas accreting towards the center during the galaxies' lifetime, and not observed at any wavelength (e.g., Peterson and Fabian, 2006)? Just $\sim$1% of the mass made available by stars is in the mass of present epoch MBHs (Ciotti and Ostriker, 2007). (2) how much radiative and mechanical energy output from the MBH can effectively interact with the surrounding ISM? (3) what are the resultant masses of the MBHs at the present epoch? and finally, (4) why bright AGNs are not common in the spheroids of the local Universe, given the expected mass accretion rate (e.g., Fabian and Canizares, 1988; Di Matteo et al., 2003; Pellegrini, 2005a)?

Recently, the interaction of the MBH with the inflowing gas has been studied with high-resolution 1D hydrodynamical simulations by Ciotti and Ostriker (2007), Ciotti et al. (2009, hereafter paper I) and Ciotti and Ostriker (2009, hereafter paper II). These simulations included a detailed and physically based treatment of the radiative energy

* Corresponding author.
E-mail address: silvia.pellegrini@unibo.it (S. Pellegrini).

0273-1177/$36.00 © 2009 COSPAR. Published by Elsevier Ltd. All rights reserved.
doi:10.1016/j.asr.2009.04.015

output from the MBH and its transfer in the ISM, and of the mechanical energy from AGN winds. They showed recurrent brief flaring of the nucleus, with the galaxy seen alternately as an AGN/starburst for a small fraction of the time and as a "normal" quiescent elliptical for much longer intervals. Accretion feedback proved effective in suppressing long lasting cooling flows and in maintaining MBH masses within the range observed today (since gas is mostly lost in outflows or starbursts); a major role in regulating the flow evolution was played also by type Ia supernovae (hereafter SNIa's).

Here, we present a preliminary investigation of the spectral and morphological appearance of this class of models in the X-ray band. In particular, we focus on the hot ISM and the nucleus during the galaxy's lifetime, both in quiescence and during outbursts of activity, and we compare their properties with the observations collected for galaxies of the local universe by *ROSAT* and more recently by *Chandra*. Section 2 briefly describes the chosen representative model, Section 3 its observational properties and a comparison with observational results, Section 4 summarizes the conclusions. We anticipate here some general results for this class of models, and a more extensive description will be given in Pellegrini, Ciotti and Ostriker (2009, hereafter paper III).

2. The representative model

The main properties of feedback modulated galactic accretion flows are given in Ciotti and Ostriker (2007) and recently in papers I and II, together with a full description of the code used for the simulations. Briefly, the code integrates the time-dependent 1D Eulerian equations of hydrodynamics, with a logarithmically spaced and staggered radial grid, extending from 2.5 pc from the central MBH to 250 kpc. The code calculates self-consistently the source and sink terms of mass, momentum and energy, associated with the evolving stellar population (stellar mass losses and SNIa's events), nuclear starbursts, accretion and MBH feedback. Gas heating and cooling are calculated for a photoionized plasma in equilibrium with an average quasar spectral energy distribution (Sazonov et al., 2005), the resulting radiation pressure and absorption/emission are computed and distributed over the ISM from numerical integration of the radiative transport equation.

Of interest here is that the adopted radiative efficiency of material accreting on the MBH at a rate $\dot{M}$ is $\epsilon = 0.1 \times 100\dot{m}/(1+100\dot{m})$, where $\dot{m} = \dot{M}/\dot{M}_{\rm Edd}$ is the Eddington-scaled accretion rate, so that $\epsilon \sim 0.1$ at large mass accretion rates (when $\dot{m} \gg 0.01$), and declines in a RIAF-like fashion $\epsilon \sim 10\dot{m}$ for $\dot{m} \lesssim 0.01$ (as for radiatively inefficient accretion flows, Narayan and Yi, 1994). The mechanical feedback implemented is that of quasar outflows (e.g., Chartas et al., 2003; Crenshaw et al., 2003), as modelled numerically by Proga (2003). The mechanical efficiency scales with the Eddington ratio ($l = L/L_{\rm Edd}$), reaching a maximum value for $l = 2$ of 3×10^{-4}–5×10^{-3} in different models. Note that only the mechanical feedback due to the Broad Line Region wind is activated (the nuclear jet properties will be inserted in a future work).

Here, we consider a representative model from the latest set of simulations (paper II), for an isolated typical elliptical galaxy with a central stellar velocity dispersion $\sigma = 260$ km s^{-1}, a B-band luminosity $L_B = 5 \times 10^{10} L_{B,\odot}$, a stellar mass described by the Jaffe law with a mass-to-light ratio $M_*/L_B = 5.8$, an effective radius $R_e = 6.9$ kpc, a dark matter halo with equal amount of dark and visible mass within R_e, a standard SNIa's rate; the maximum value of the mechanical efficiency is set to 10^{-3}. The simulations begin at a galaxy age of $\sim$2 Gyr (i.e., a redshift $z \sim 2$, the exact value depending on the epoch of elliptical galaxy formation, usually put at $z \gtrsim 2$) and soon AGN outbursts develop, each followed by an abrupt drop of the accretion rate, and by times during which the galaxy is replenished of gas by the stellar mass losses.

The typical behavior of the gas during an outburst starts with the off-center growth of a shell of denser gas (at a radius of $\sim$0.5–1 kpc) that progressively cools, falls and reaches the center (i.e., a cooling collapse occurs). Then a radiative shock quickly [in $\sim(1$–$2) \times 10^6$ yr] produces an outward moving shell of cold and dense gas, that slows down until it falls back towards the center, accumulating far more material than the first shell, and giving origin to a larger accretion and feedback episode. After some more events of this kind, a major shock leaves behind a very hot and dense center, and causes substantial galaxy degassing. The gas then cools and resumes its subsonic velocity, the density starts increasing again and the cycle repeats. Overall, during outbursts both hotter and colder regions are continuously created, the hotter ones mainly at the center (due to gas compressed by the falling shells, or to shocks) and the colder ones due to the gas in the falling shells or in the radiative shocks.

We remark that the representative model has fairly standard input parameter values, and its general properties described below are typical of this class of models. A large set of runs exploring the impact of different values for the feedback parameters (e.g., the wind opening angle, the peak mechanical efficiency and its dependence on l) showed present-day properties similar to those of the adopted representative model (papers I and II).

3. Comparison of simulated and observed X-ray properties

We consider in turn the evolution of the luminosity of the nucleus (Section 3.1), of the total luminosity and emission weighted temperature of the hot gas (Section 3.2), of the temperature profile (Section 3.3) and of the surface brightness profile (Section 3.4). The emission is calculated over the full *Chandra* sensitivity band (0.3–8 keV), and in two separate bands, 0.3–2 and 2–8 keV, by means of the APEC code within the package XSPEC for the X-ray data analysis (see paper III for more details).

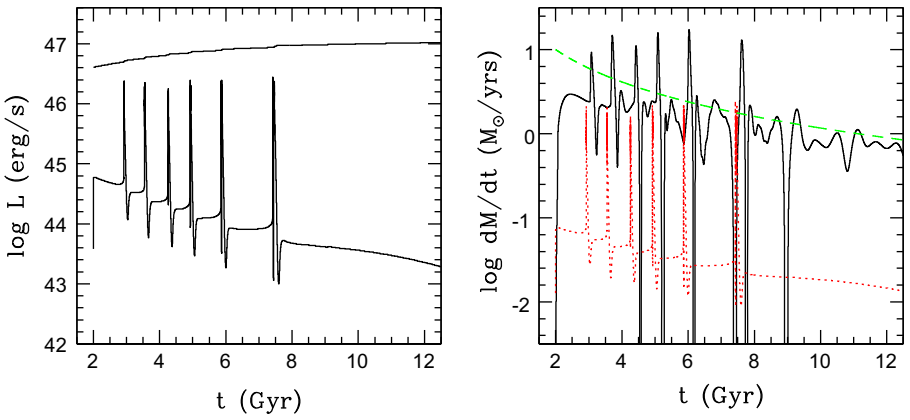

Fig. 1. Left panel: the evolution of the bolometric luminosity produced by nuclear accretion. The upper line is the Eddington luminosity (note the slow and overall modest increase of the MBH mass). Right panel: the evolution of the mass budget: the stellar mass loss rate (green line), the gas mass leaving the galaxy at a radius of $10R_e$ (black line) and the mass accretion rate on the MBH (red line). (For interpretation of the references to color in this figure legend, the reader is referred to the web version of this paper.)

Since in the simulations the treatment of feedback is physically based, not arbitrarily chosen and tuned to reproduce observations, any agreement or discrepancy of the resulting model properties with observations is relevant to improve our understanding of the MBH–ISM coevolution.

3.1. The nuclear luminosity

The time evolution of the bolometric nuclear luminosity shows strong intermittencies at an earlier epoch, reaching the Eddington value, and becoming rarer and rarer with time, until a smooth, very sub-Eddington phase establishes (Fig. 1). This behavior follows from the secular decrease of the stellar mass loss rate (Fig. 1), which produces longer and longer times for the replenishment of the galaxy with gas. Towards the present epoch (a galaxy age of ~12 Gyr) the mass accretion rate is $\dot{M} \sim 0.01 M_\odot$/yr, that is $\dot{m} \sim 1.1 \times 10^{-3}$, therefore accretion has entered the RIAF regime and $\epsilon \simeq 0.01$ (Section 2). The nuclear bolometric luminosity is $L_{\rm bol} = 2 \times 10^{43}$ erg s^{-1} and its $l = 2 \times 10^{-4}$, in agreement with the fact that in the local universe the fraction of MBHs approaching their Eddington limit is negligible. For example, in the statistically complete Palomar spectroscopic survey of 486 nearby galaxies only ~50% of ellipticals show emission line nuclei, mostly of low level ($L_{H\alpha} < 10^{40}$ erg s^{-1}); for LINERs, a sub-sample largely dominated by ellipticals, $L_{\rm bol}$ ranges from 10^{39} to 10^{43} erg s^{-1}, with a peak at $L_{\rm bol} \sim 10^{41}$ erg s^{-1}, and the median[1] $l = (0.5 - 1) \times 10^{-5}$ (Ho, 2008). Seyferts excluded, nuclei of all types have $L_{\rm bol} < 10^{43}$ erg s^{-1}. Therefore the representative model may need a reduction of its $L_{\rm bol}$, in addition to that produced by the adopted low radiative efficiency of RIAFs, to be more representative of the typical low luminosity nucleus of the local universe.

Indeed, many nuclei of nearby ellipticals studied in detail in the X-ray band show emission at an extremely low level. Their 0.3–10 keV luminosities $L_{X,\rm nuc}$, for a sample within ~50 Mpc, with or without radio emission and residing in all kinds of environments, range from few $\times 10^{38}$ erg s^{-1} to $\sim 10^{42}$ erg s^{-1}, with $L_{X,\rm nuc}/L_{\rm Edd}$ as low as 10^{-6}–10^{-8} the most common (Pellegrini, 2005a,b; see also Soria et al., 2006; Gallo et al., 2008). $L_{X,\rm nuc}$ of the model at the present epoch can be derived from $L_{\rm bol}$ adopting a correction factor appropriate for the spectral energy distribution of a RIAF, that is $\lesssim 0.2$ for low luminosity MBHs (Mahadevan, 1997). This gives $L_{X,\rm nuc} \lesssim 4 \times 10^{42}$ erg s^{-1}, and $L_{X,\rm nuc}/L_{\rm Edd} \lesssim 4 \times 10^{-5}$, both values again quite higher than typically observed.

A reduction of the model nuclear luminosity could be accomplished by inserting the mechanical feedback[2] of a jet or of a nuclear wind, that should naturally develop in low radiative efficiency accretion (Blandford and Begelman, 1999), and should reduce further the mass accretion rate (e.g., Di Matteo et al., 2003). In fact, the Bondi accretion rate for the hot ISM around many nearby MBHs, coupled to the RIAF radiative efficiency, corresponds to luminosities still higher than observed, indicating the need for a reduction of the mass that actually reaches the MBH (Loewenstein et al., 2001; Pellegrini, 2005a; Pellegrini et al., 2007a,b). Another indication of the relevance of mechanical feedback is the observed link between the radio luminosity and the X-ray gas asymmetry index for ~50 nearby ellipticals (Diehl and Statler, 2008a).

Finally, note that $L_{X,\rm nux}$ is observed to be independent of the MBH mass and of the Bondi accretion rate (Pellegrini, 2005a). Likely, neither Bondi accretion nor simple RIAFs realistically describe the interaction between the outgoing

[1] $L_{\rm bol}$ derives from the nuclear 2–10 keV emission, with $L_{\rm bol}/L_{2-10keV} = 16$ as appropriate for low luminosity AGNs, and $L_{\rm Edd}$ from MBH masses estimated from the MBH–σ relation.

[2] We recall that the simulations include only the mechanical feedback due to the Broad Line Region wind (see Section 2 and Fig. 1 in paper I).

energy flux and the incoming mass flux at the nucleus, while the fluctuations typical of feedback cycles can account for the observed lack of relationship.

3.2. Global gas luminosity and temperature

The time evolution of the gas emission shows peaks during outbursts, that become broader and less high with time increasing (Fig. 2). Soft and hard emission oscillate in phase and present the same overall behavior, with the hard one keeping $\lesssim$100 times lower. Hard emission during outbursts would be difficult to distinguish from the contribution of unresolved binaries even with *Chandra*, if extended (e.g., Trinchieri et al., 2008), but it could be detected if centrally concentrated (see also Section 3.4).

The largest compilation of the global X-ray emission of early type galaxies of the local universe is based on *ROSAT* observations of a relatively unbiased sample of 401 objects, homogeneously analyzed (O'Sullivan et al., 2001). The best fit correlation with the B-band luminosity of the emission mostly due to hot gas ($L_{X,\rm ISM}$), after subtraction of the stellar contribution, predicts $L_{X,\rm ISM} \sim 10^{41}$ erg s^{-1} for $L_B = 5 \times 10^{10} L_{B,\odot}$ as the model galaxy. However at this L_B, due to the large scatter around the best fit, the observed $L_{X,\rm ISM}$ ranges from 10^{40} erg s^{-1} up to few $\times 10^{42}$ erg s^{-1} (though $L_{X,\rm ISM}>$ few $\times 10^{41}$ erg s^{-1} belong to galaxies with an important contribution from the intragroup or intracluster medium). At an age of ~10–12 Gyr the model has $L_{X,\rm ISM} \sim 10^{40}$ erg s^{-1} (Fig. 2), on the lower end of the observed range. This indicates that degassing is too efficient in the simulations, at least at the present epoch. This problem would be alleviated by an external pressure from an outer medium (e.g., Vedder et al., 1988), a more appropriate "boundary" in fact for ellipticals that usually are not isolated (it will be considered in future simulations).

The lower panel of Fig. 2 shows the evolution of the soft ($\langle T\rangle_s$) and hard ($\langle T\rangle_h$) emission weighted temperatures within the optical R_e, and their complex behavior during outbursts. The sharp and high peaks in $\langle T\rangle_h$ correspond to the onset of very hot regions, while the decrements in $\langle T\rangle_s$ are due to a dense cold shell preceding the major burst and to cold gas swept by the radiative shocks produced by the outburst (see Section 2). The 0.3–8 keV emission weighted temperature (not shown in Fig. 2) is almost coincident with $\langle T\rangle_s$, except for those short times with a very hot gas component.

ROSAT observations showed a correlation, though with a large degree of scatter, between the temperature weighted with the soft emission of the whole galaxy (T) and the central σ (O'Sullivan et al., 2003), predicting $T \sim 0.7$ keV (with observed values from ~0.4 to ~1 keV) for $\sigma = 260$ km s^{-1} as for the model galaxy. At the present epoch the model has $T \sim 0.5$ keV, lower than the best fit prediction but within the observed range, and $\langle T\rangle_s = 0.7$ keV (Fig. 2). Likely the observed T refers to a region less extended radially (and typically also hotter) than used for the model galaxy. Average temperatures within R_e have been obtained with *Chandra* (Athey, 2007), whose high angular resolution allows for a better subtraction of the point (stellar) source contribution and then gas temperatures closer to the true ones. For 22 Athey's galaxies with $\log L_B = 10.5$–10.8, similar to that of the model, the average 0.3–8 keV emission weighted temperature is 0.60 keV, close to $\langle T\rangle_s$ though slightly lower.

Summarizing, the gas content of the model is lower than the average observed for a galaxy of its size; this shows the need for a lower SNIa heating, or a higher/more concentrated gravitating mass, or the confining effect of an external medium. The average temperatures instead agree reasonably with observations, and modifications to the

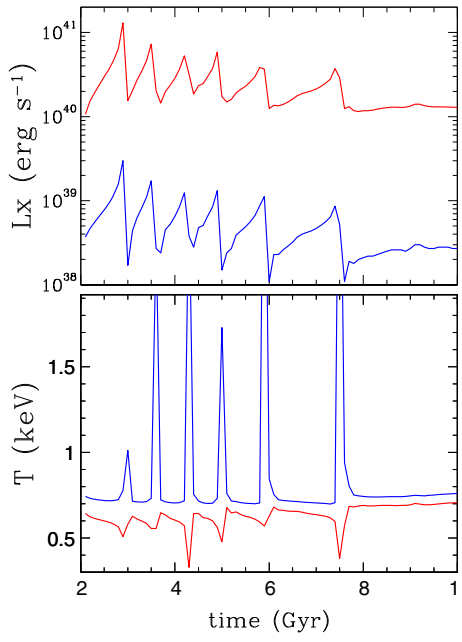

Fig. 2. Time evolution of the total gas luminosity and emission weighted temperature within the optical effective radius R_e, in the 0.3–2 keV band (red lines) and in the 2–8 keV band (blue lines). (For interpretation of the references to color in this figure legend, the reader is referred to the web version of this paper.)

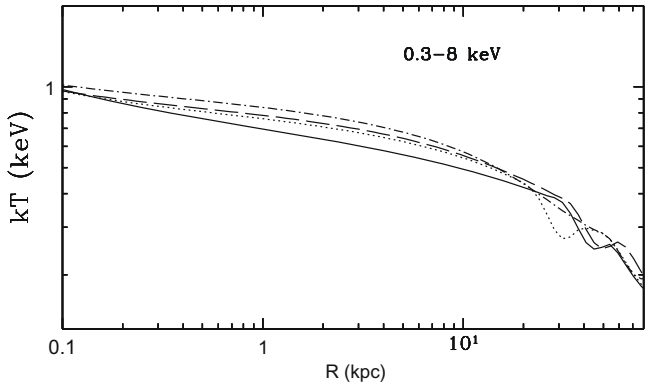

Fig. 3. Projected temperature profiles weighted with the emission in the 0.3–8 keV band, during the inter-burst times $t = 6.9$ Gyr (solid line), 8.1 Gyr (dotted), 9.1 Gyr (dashed) and 11.1 Gyr (dot-dashed line).

model should not increase the average temperature within R_e, while they could increase a little that over the whole galaxy.

3.3. Temperature profiles

The emission-weighted and projected temperature profiles are shown during quiescent inter-burst periods in Fig. 3, and during the last outburst at ~7.5 Gyr in Fig. 4. During quiescent times the profiles are smooth, with the temperature monothonically decreasing for increasing radius (from ~1 keV at a radius of ~100 pc to ~0.4–0.5 keV at ~20 kpc). Negative temperature gradients are typical of inflowing gas in steep potentials (e.g., Pellegrini and Ciotti, 1998), just due to compressional heating. Diehl and Statler (2008b) suggest that negative temperature gradients could be the sign of localized heating by a central, weak AGN. In fact in the models, even during quiescent times, accretion is present (though with a low radiative efficiency, Sections 2 and 3.1), and this has an additional heating effect over gravitational compression on the gas at the center. Negative gradients are commonly observed among ellipticals, as revealed by *Chandra* for an increasing number of galaxies (Fukazawa et al., 2006; Athey, 2007; Diehl and Statler, 2008b), and the temperature roughly halves from the center to the galaxy outskirts, as in the model. A few galaxies have central temperatures of ~1 keV (as in Fig. 3), while most show temperatures between 0.5 and 1 keV at their innermost radial bin. However, the model temperature calculated as an average for a central bin extending out to 0.5 – a few kpc, as for observed galaxies, will be lower than 1 keV. While a more detailed comparison is postponed to paper III, we conclude here that no additional heating seems to be required in the central region (as found in Section 3.2).

In other observed profiles the temperature increases outward, or keeps roughly flat, or is "hybrid", firstly decreasing from the central value to a minimum and then increasing out to the edge of the galaxy (Diehl and Statler, 2008b). These profiles could be produced in the model by environmental effects currently not included (e.g., Vedder et al., 1988; Mathews and Brighenti, 2003). A temperature decreasing towards the center is also observed, but is never shown by the model during quiescence. A central drop in temperature and a shape resembling the hybrid profile are shown during particular phases of outbursts, when the major shock is moving outwards or the cold shell is forming (see Fig. 4 that illustrates the messy temperature distribution during the ~0.2 Gyr of an outburst, consequent to the gas flow behavior described in Section 2).

We noted (Section 3.1) that the stationary hot accretion phase needs a reduction of the accretion rate, as can be provided by a jet. In a recent *Chandra* analysis the temperature profiles outside $\sim R_e$ showed gradients that switch monothonically from positive to negative going from high to low radio luminosities within three R_e (Diehl and Statler, 2008b). To be consistent with this result, the jet addition to the simulations should heat the gas outside $\sim R_e$.

Finally note that the temperature profile of the elliptical NGC3411 shows an intriguing off-center dip (O'Sullivan et al., 2007) that is highly unusual for standard cooling flow models but is present in a few profiles in Fig. 4. This dip corresponds to a ripple in the observed X-ray brightness

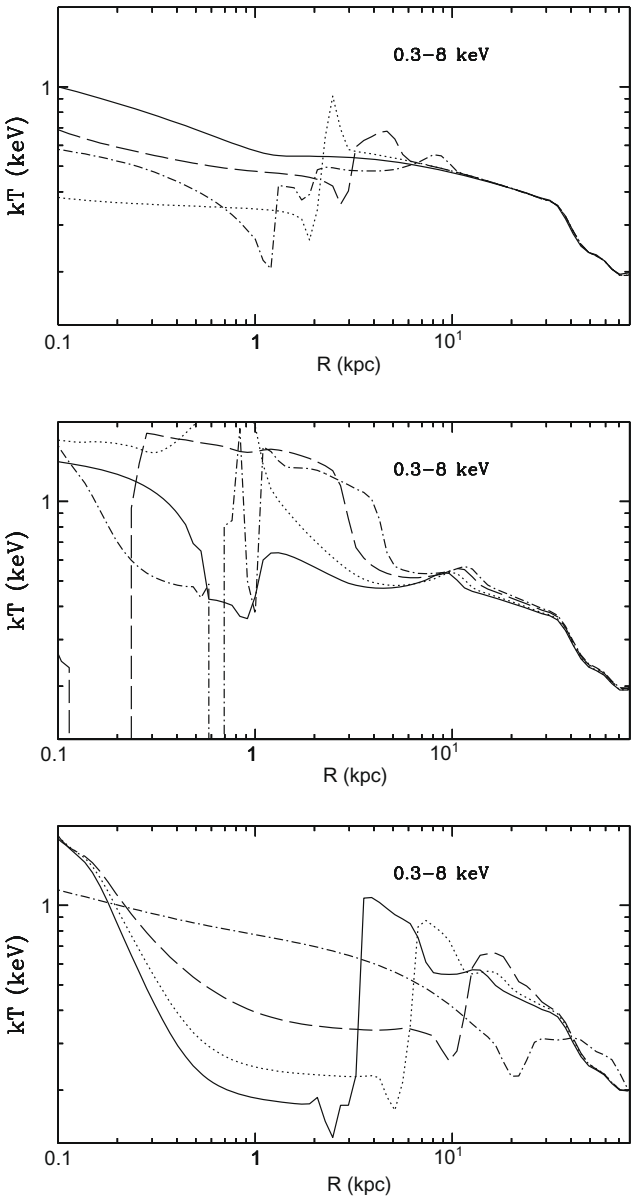

Fig. 4. Projected temperature profiles for the gas emission during the last outburst (see Section 2 for more details). Upper panel: the shell is forming at a radius of ~1 kpc and approaching the center (solid line); a shock is moving outward after the first burst (dotted line, after 54 Myr; dashed line, after 4 Myr), creating a major shell that falls back to the center (dot-dashed line, after 8 Myr). Central panel (the time step between each line is 2 Myr): after the shell has reached the center, a shock is moving outward, creating a central very hot bubble (solid line, dotted line), that quickly cools (dashed and dot-dashed line). Bottom panel: the shock is moving outwards [solid (+4 Myr), dotted (+6 Myr), dashed (+16 Myr) lines]; quiescence is resuming (dot-dashed line, +0.1 Gyr). The time elapsed from the beginning of the outburst (Fig. 4, upper panel, solid line) is 0.2 Gyr.

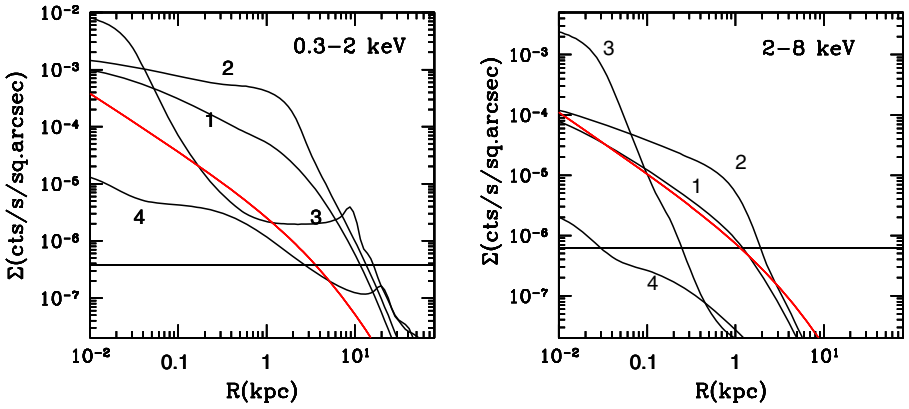

Fig. 5. The brightness profile during the last major outburst; curves referring to subsequent times are labelled from 1 to 4 (see Section 3.4 for a description of the main features). Count rates in the *y*-axis and background level (straight horizontal line) are for the *Chandra* ACIS-S detector. The red line shows the profile of unresolved X-ray binaries, appropriate for their spectral shape and a representative observation of a Virgo galaxy with an exposure of 200 ks (e.g., Kim et al., 2006). (For interpretation of the references to color in this figure legend, the reader is referred to the web version of this paper.)

profile, that is also a frequent feature in the model (Section 3.4).

3.4. Brightness profiles

The evolution of the surface brightness profile is shown in Fig. 5, right before and during the last major outburst, and in Fig. 6, during the subsequent slow evolution until the present epoch quiescent state. In Fig. 5 curves labelled 1 and 2 show two subsequent times of the off-center shell formation, lasting $\sim$0.5 Gyr. Curve labelled 3 shows a shock moving outwards after the major outburst (in the upper panel) and the presence of very hot gas at the center (lower panel); this phase lasts for $\sim 2\times10^7$ yr. Curve labelled 4 shows the result of the degassing caused by the passage of the shock waves: the galaxy has a low gas density and subsonic perturbations remain at a radius of a few tens of kpc; the time is $\lesssim$0.2 Gyr since the outburst started. Note how the main features in the profile are above the levels of background and of unresolved stellar emission (described in the caption of the figures). The high-temperature, high-density phase at the center (curve 3) is very brief, and unlikely to be observed. Disturbances as shells and ripples lasting $\lesssim$0.2 Gyr are more likely to be observed. In fact, many nearby galaxies show these characteristics in their images, as recently proven with *Chandra* studies (Diehl and Statler, 2008a; Machacek et al., 2006).

Interestingly, three bright ellipticals imaged with *Chandra* (Loewenstein et al., 2001) all show a flattish X-ray brightness profile within the central 3–10 arcsec ($\lesssim$1 kpc), that is not possible to reproduce with inflow models, while it resembles the profile of the "pre-burst"phase (curves 1 and 2 in Fig. 5).

4. Summary and conclusions

We have calculated the X-ray properties of a galaxy model representative of a recent investigation of feedback modulated accretion including the combined heating of radiation and AGN winds (papers I and II), and we have compared them with observations of the local universe. Besides important achievements as limiting the growth of the MBH mass to observed values (papers I and II), thanks to the present analysis these models also reveal important aspects of the MBH–ISM coevolution, as detailed below.

At the present epoch a highly sub-Eddington ($l\sim10^{-4}$) phase establishes with accretion in the low radiative efficiency regime. Though within the range observed, the nuclear emission is quite larger than the most frequently observed values [$l\sim(0.5-1)10^{-5}$]. This suggests that an additional mechanism reducing further the mass available for accretion is important, as could be provided by a nuclear jet or wind from a RIAF.

During the many outbursts, the gas emission $L_{X,\mathrm{ISM}}$ presents peaks that become broader as time increases; sharp peaks and decrements are shown respectively by the hard and soft emission weighted temperature. At the final quiescent times, $L_{X,\mathrm{ISM}}$ is on the lower side of those observed,

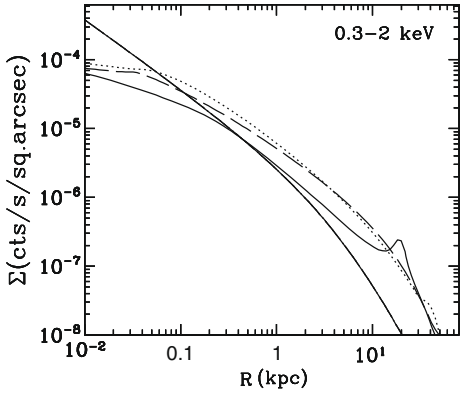

Fig. 6. The evolution of the brightness profile after the last major outburst: the quiescent state establishes again and is kept until the end of the simulation. The solid, dotted, dashed lines correspond to times of 7.7, 8.7 and 10.0 Gyr. Count rates and unresolved stellar emission profile (thin smoother line) have been calculated as for Fig. 5.

which suggests degassing may be less efficient, or the confining agents (gravitating mass, external medium) more efficient. The emission weighted temperatures instead compare well with observations.

The profiles of brightness and temperature (decreasing outward) in quiescence resemble those of many local galaxies. Outbursts produce features in the brightness profile that are detectable with *Chandra*, last for $\lesssim 0.2$ Gyr, and could match part of the widespread gas disturbances observed in local galaxies. The hot bubbles inflated at the center produce central peaks in the hard band brightness profile, but their short duration makes them difficult to observe.

In conclusion, a form of feedback lowering further the nuclear luminosity during the stationary hot accretion phase seems important. This should not increase the central temperature that is already consistent with observed values. A jet interacting mainly outside ~ 0.5–$1 R_e$ would then be preferable; it should also heat the gas there, to bring the overall temperature profile in accord with those observed (increasing outward) at high radio luminosities. The additional feedback should not lower $L_{X,\mathrm{ISM}}$.

Finally, we comment on how $L_{X,\mathrm{ISM}}$ and the gas temperature might scale with galaxy properties, and with how much scatter. A change of the mass content and distribution, SNIa rate and external pressure will have an impact on the gas content, and also on the possibility of having outbursts until the present epoch, or no outbursts at all. For example, the SNIa heating may keep small galaxies in an outflow so that outbursts never happen; due to a larger dark matter content, galaxies as the representative model may never experience a huge degassing, and may host nuclear outbursts until the present epoch. In general, we expect a trend of $L_{X,\mathrm{ISM}}$ with L_B mainly determined by the galaxy structure and SNIa's heating, as described by older studies (e.g., Pellegrini and Ciotti, 1998), to which scatter is added by feedback, but only for luminous galaxies (as the representative model). The frequency of outbursts at the present epoch is difficult to estimate, given the many parameters involved, but it should be very small (papers I and II). The hot gas disturbances shown by *Chandra* have been mostly attributed to an ongoing or recent jet activity (e.g., Diehl and Statler, 2008a,b), though evidence for this is not always present (e.g., NGC4552, Machacek et al., 2006). A statistically complete sample of galaxies with information on the nature of activity and of the gas disturbances will hopefully be built soon from the large *Chandra* database.

References

Athey, A.E. Chandra Observations of Early-type Galaxies, Ph.D. Thesis. University of Michigan. Available from: <arXiv:0711.0395> (Chapter IV)..

Blandford, R., Begelman, M.C. On the fate of gas accreting at a low rate on to a black hole. MNRAS 303, L1–L5, 1999.

Chartas, G., Brandt, W.N., Gallagher, S.C. XMM-Newton reveals the quasar outflow in PG 1115+080. ApJ 595, 85–93, 2003.

Ciotti, L., D'Ercole, A., Pellegrini, S., Renzini, A. Winds, outflows and inflows in X-ray elliptical galaxies. ApJ 376, 380–403, 1991.

Ciotti, L., Ostriker, J.P. Radiative feedback from massive black holes in elliptical galaxies: AGN flaring and central starburst fueled by recycled gas. ApJ 665, 1038–1056, 2007.

Ciotti, L., Ostriker, J.P., Proga, D. Feedback from central black holes in elliptical galaxies. I: models with either radiative or mechanical feedback but not both. ApJ, in press. Available from: <arXiv:0901.1089> (paper I).

Ciotti, L., Ostriker, J.P. Feedback from central black holes in elliptical galaxies. III: models with both radiative and mechanical feedback. ApJ, submitted for publication (paper II).

Crenshaw, D.M., Kraemer, S.B., George, I.M. Mass loss from the nuclei of active galaxies. ARAA 41, 117–167, 2003.

David, L.P., Forman, W., Jones, C. Evolution of the interstellar medium in elliptical galaxies. II – X-ray properties. ApJ 369, 121–134, 1991.

Diehl, S., Statler, T.S. The hot interstellar medium of normal elliptical galaxies. II. Morphological evidence for active galactic nucleus feedback. ApJ 680, 897–910, 2008a.

Diehl, S., Statler, T.S. The hot interstellar medium in normal elliptical galaxies. III. The thermal structure of the gas. ApJ 687, 986–996, 2008b.

Di Matteo, T., Allen, S.W., Fabian, A.C., Wilson, A.S., Young, A.J. Accretion onto the supermassive black hole in M87. ApJ 582, 133–140, 2003.

Di Matteo, T., Springel, V., Hernquist, L. Energy input from quasars regulates the growth and activity of black holes and their host galaxies. Nature 433, 604–607, 2005.

Fabian, A.C., Canizares, C.R. Do massive black holes reside in elliptical galaxies?. Nature 333, 829–831, 1988.

Ferrarese, L., Merritt, D. A fundamental relation between supermassive black holes and their host galaxies. ApJ 539, L9–L12, 2000.

Fukazawa, Y., Botoya-Nonesa, J.G., Pu, J., Ohto, A., Kawano, N. Scaling mass profiles around elliptical galaxies observed with Chandra and XMM-Newton. ApJ 636, 698–711, 2006.

Gallo, E., Treu, T., Jacob, J., Woo, J.-H., Marshall, P.J., Antonucci, R. AMUSE-Virgo. I. Supermassive black holes in low-mass spheroids. ApJ 680, 154–168, 2008.

Gebhardt, K., Bender, R., Bower, G., et al. A relationship between nuclear black hole mass and galaxy velocity dispersion. ApJ 539, L13–L16, 2000.

Ho, L.C. Nuclear activity in nearby galaxies. ARAA 46, 475–539, 2008.

Hopkins, P.F., Hernquist, L., Cox, T.J., Di Matteo, T., Robertson, B., Springel, V. A unified, merger-driven model of the origin of starbursts, quasars, the cosmic X-ray background, supermassive black holes, and galaxy spheroids. ApJS 163, 1–49, 2006.

Kim, D.W., Fabbiano, G., Kalogera, V., et al. Probing the low-luminosity X-ray luminosity function in normal elliptical galaxies. ApJ 652, 1090–1096, 2006.

Kormendy, J., Fisher, D.B., Cornell, M.E., Bender, R. Structure and formation of elliptical and spheroidal galaxies. ApJS, in press. Available from: <arXiv:0810.1681>.

Loewenstein, M., Mushotzky, R.F., Angelini, L., Arnaud, K.A., Quataert, E. Chandra limits on X-ray emission associated with the supermassive black holes in three giant elliptical galaxies. ApJ 555, L21–L24, 2001.

Machacek, M., Nulsen, P.E.J., Jones, C., Forman, W.R. Chandra observations of nuclear outflows in the elliptical galaxy NGC 4552 in the Virgo cluster. ApJ 648, 947–955, 2006.

Mahadevan, R. Scaling laws for advection-dominated flows: applications to low-luminosity galactic nuclei. ApJ 477, 585–601, 1997.

Mathews, W., Brighenti, F. Hot gas in and around elliptical galaxies. ARA&A 41, 191–239, 2003.

Merloni, A., Rudnick, G., Di Matteo, T. Tracing the cosmological assembly of stars and supermassive black holes in galaxies. MNRAS 354, L37–L42, 2004.

Narayan, R., Yi, I. Advection-dominated accretion: a self-similar solution. ApJ 428, L13–L16, 1994.

O'Sullivan, E., Forbes, D., Ponman, T. A catalogue and analysis of X-ray luminosities of early-type galaxies. MNRAS 328, 461–484, 2001.

O'Sullivan, E., Ponman, T.J., Collins, R.S. X-ray scaling properties of early-type galaxies. MNRAS 340, 1375–1399, 2003.

O'Sullivan, E., Vrtilek, J.M., Harris, D.E., Ponman, T.J. On the anomalous temperature distribution of the intergalactic medium in the NGC 3411 group of galaxies. ApJ 658, 299–313, 2007.

Pellegrini, S., Ciotti, L. Decoupled hot gas flows in elliptical galaxies. A&A 333, 433–444, 1998.

Pellegrini, S. Nuclear accretion in galaxies of the local Universe: clues from Chandra observations. ApJ 624, 155–161, 2005a.

Pellegrini, S. The X-ray emission properties and the dichotomy in the central stellar cusp shapes of early-type galaxies. MNRAS 364, 169–178, 2005b.

Pellegrini, S., Baldi, A., Kim, D.W., Fabbiano, G., Soria, R., Siemiginowska, A., Elvis, M. A deep Chandra look at the low-LB elliptical NGC 821: X-ray binaries, a galactic wind, and emission at the nucleus. ApJ 667, 731–748, 2007a.

Pellegrini, S., Siemiginowska, A., Fabbiano, G., Elvis, M., Greenhill, L., Soria, R., Baldi, A., Kim, D.W. A deep Chandra, VLA and Spitzer IRAC study of the very low luminosity nucleus of the elliptical NGC 821. ApJ 667, 749–759, 2007b.

Peterson, J.R., Fabian, A.C. X-ray spectroscopy of cooling clusters. Phys. Rep. 427, 1–39, 2006.

Proga, D. Numerical simulations of mass outflows driven from accretion disks by radiation and magnetic forces. ApJ 585, 406–417, 2003.

Sazonov, S.Yu., Ostriker, J.P., Ciotti, L., Sunyaev, R.A. Radiative feedback from quasars and the growth of massive black holes in stellar spheroids. MNRAS 358, 168–180, 2005.

Soria, R., Graham, A., Fabbiano, G., Baldi, A., Elvis, M., Jerjen, H., Pellegrini, S., Siemiginowska, A. Accretion and nuclear activity of quiescent supermassive black holes. II: optical study and interpretation. ApJ 640, 143–155, 2006.

Trinchieri, G., Pellegrini, S., Fabbiano, G., Fu, R., Brassington, N.J., Zezas, A., Kim, D.-W., Gallagher, J., Angelini, L., Davies, R.L. Discovery of hot gas in outflow in NGC 3379. ApJ 688, 1000–1008, 2008.

Vedder, P.W., Trester, J.J., Canizares, C.R. Models of steady state cooling flows in elliptical galaxies. ApJ 332, 725–751, 1988.